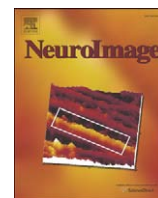




Contents lists available at ScienceDirect

NeuroImage

journal homepage: www.elsevier.com/locate/ynimg

Whole brain quantitative T2 MRI across multiple scanners with dual echo FSE: Applications to AD, MCI, and normal aging[☆]

Corinna M. Bauer^a, Hernán Jara^{b,c}, Ron Killiany^{a,d,e,*}
and Alzheimer's Disease Neuroimaging Initiative

^a Department of Anatomy and Neurobiology, Boston University School of Medicine, 700 Albany Street, W701 Boston, MA 02118, USA

^b Department of Radiology, Boston Medical Center, Boston University School of Medicine, 820 Harrison Avenue, Boston, MA 02118, USA

^c Department of Biomedical Engineering, Boston University, 44 Cummings Street, Boston, MA 02215, USA

^d Center for Biomedical Imaging, Boston University School of Medicine, 650 Albany Street, Boston, MA 02118, USA

^e Department of Environmental Health, Boston University School of Public Health, 715 Albany Street, Boston, MA 02118, USA

ARTICLE INFO

Article history:

Received 31 August 2009

Revised 26 April 2010

Accepted 27 April 2010

Available online xxx

ABSTRACT

The ability to pool data from multiple MRI scanners is becoming increasingly important with the influx in multi-site research studies. Fast spin echo (FSE) dual spin echo sequences are often chosen for such studies based principally on their short acquisition time and the clinically useful contrasts they provide for assessing gross pathology. The practicality of measuring FSE-T2 relaxation properties has rarely been assessed. Here, FSE-T2 relaxation properties are examined across the three main scanner vendors (General Electric (GE), Philips, and Siemens). The American College of Radiology (ACR) phantom was scanned on four 1.5 T platforms (two GE, one Philips, and one Siemens) to determine if the dual echo pulse sequence is susceptible to vendor-based variance. In addition, data from 85 subjects spanning the spectrum of normal aging, mild cognitive impairment (MCI), and Alzheimer's disease (AD) was obtained from the Alzheimer's Disease Neuroimaging Initiative (ADNI) to affirm the presence of any phantom based between vendor variance and determine the relationship between this variance and disease. FSE-T2 relaxation properties, including peak FSE-T2 and histogram width, were calculated for each phantom and human subject. Direct correspondence was found between the phantom and human subject data. Peak FSE-T2 of Siemens scanners was consistently at least 20 ms prolonged compared to GE and Philips. Siemens scanners showed broader FSE-T2 histograms than the other scanners. Greater variance was observed across GE scanners than either Philips or Siemens. FSE-T2 differences were much greater with scanner vendor than between diagnostic groups, as no significant changes in peak FSE-T2 or histogram width between normal aged, MCI, and AD subject groups were observed. These results indicate that whole brain histogram measures are not sensitive enough to detect FSE-T2 changes between normal aging, MCI, and AD and that FSE-T2 is highly variable across scanner vendors.

© 2010 Published by Elsevier Inc.

Alzheimer's disease (AD) is a progressive neurodegenerative disorder characterized by an insidious onset followed by gradual decline in cognitive function. It is the most common form of dementia and is quickly becoming a global crisis, affecting approximately 10% of individuals over age 65 and nearly 50% of individuals over 85 years of age (Evans et al., 1989). An additional 19% of individuals over age

65, and 29% over age 85, are estimated to have mild cognitive impairment (MCI) (Lopez et al., 2003). MCI represents the transitional phase between normal aging and probable AD, whereby individuals have diminished memory function, yet maintain normal levels of daily activity and are not demented (Petersen et al., 2001). Individuals with the amnesic form of MCI are more likely to develop AD than their normal counterparts; those with amnesic MCI show rates of conversion around 12% per year, whereas normal elderly tend to convert to AD at 1–2% a year (Petersen et al., 1999). With the development of potential therapeutic interventions it is becoming important to identify potential biomarkers of disease presence as early as possible.

Tissue relaxation properties as measured with quantitative T2 MRI have the potential to be a valuable resource in early identification of individuals with MCI and AD. T2 is a function of tissue free water properties and the local environment of the nuclei, allowing one to

[☆] Data used in the preparation for this article were obtained from the Alzheimer's Disease Neuroimaging Initiative (ADNI) database (<http://www.loni.ucla.edu/ADNI>). As such, the investigators within the ADNI contributed to the design and implementation of ADNI and/or provided data, but did not participate in analysis or writing of this manuscript. A complete listing of ADNI investigators can be found at http://www.loni.ucla.edu/ADNI/Collaboration/ADNI_Citation.shtml.

* Corresponding author. Boston University School of Medicine, 700 Albany Street, Room W-701, Boston, MA 02118, USA. Fax: +1 617 638 4922.

E-mail address: killiany@bu.edu (R. Killiany).

examine tissue state and hydration (Jack, 1996). The neuropathology of MCI and AD both involve the deposition of neurofibrillary tangles and amyloid plaques. These entities result in neuronal loss and may affect the relaxation properties of the surrounding tissue, which in turn may alter the T2 times. Histological studies suggest that iron and water content increase in AD brains, resulting in shortened and prolonged T2 values, respectively (Schenck et al., 2006), as T2 is sensitive to iron levels in brain tissue (Vymazal et al., 1996; Bartzokis et al., 1997). Because quantitative T2 values reflect tissue characteristics, it may be useful to study neuronal degradation in AD prior to other detectable atrophy.

Most previous research on T2 relaxation in AD has been conducted at a single research center using data collected on a single scanner. Given the current trend for conducting multi-site studies and for individual sites to have multiple scanners, often from different vendors, it is beneficial to examine T2 relaxation properties in a multi-vendor research study. Multi-site investigations enable a larger recruitment population than at a single site; however, studies using imaging information obtained at multiple sites have the added difficulty of ensuring consistent results between sites. Of importance to this study are potential differences in the fast (a.k.a. turbo) spin echo (FSE) readouts used with the 2D-FSE pulse sequence. It has been shown using voxel-based morphometry (VBM) that the effect of disease on regional brain volume may be greater than the effect of scanner variation in a population of AD and normal aged subjects across six scanners (Stonnington et al., 2008). The current study will examine if the same holds true for FSE-T2 relaxation. It should be noted that there are a number of ways to measure T2 and the results of each method are likely to be dependent upon the sequence used. For the purposes of clarity in this manuscript we will be referring to T2 as FSE-T2 in order to reflect the methodology/sequence that was used to measure it.

Prior studies on scanner variability have focused on volumetric measures, primarily derived from T1-weighted pulse sequences. Image uniformity, geometry (Ihalainen et al., 2004; Fu et al., 2006), and signal to noise ratio (Fu et al., 2006) have been shown to vary both within and between vendors and platforms; but, no studies have examined quantitative T2 using fast spin echo sequences across multiple vendors or platforms. Since no sequences are standardized between vendors, it is unknown if the acquired FSE-T2 values are similar or different, and to what degree they may be different. One relaxometry study that was conducted across three research sites using GE and Siemens platforms has shown minimal variance due to a scanner using the DESPOT2 (driven equilibrium single pulse observation of T2) pulse sequence (Deoni et al., 2008). In the present study we tested if the dual echo FSE pulse sequence showed similar accuracy between scanner vendors using both the ACR phantom and human subjects. It should be noted that specific pulse sequence parameters are often slightly different between scanner vendors and platforms in multi-site imaging studies in order to produce images with similar image quality and appearance. It is unclear how these pulse sequence variations between vendors affect FSE-T2 values. This paper seeks to quantify these potential discrepancies.

The specific aim of the current study was to assess the FSE-T2 values obtained from MRI scans of phantoms and the human brain on either GE, Philips, or Siemens scanners. We used ACR phantom scans from four MRI scanners and human MRI data acquired from the Alzheimer's Disease Neuroimaging Initiative (ADNI) database, incorporating multiple platforms from three manufacturers. The human subjects fell into the categories of normal aging (NL), MCI or AD groups. In this context, the purposes of this work were: first, to study possible vendor-dependent systematic differences in FSE-T2 in the ACR phantom and human subjects, and second, to explore possible FSE-T2 histogram signatures of normal aging, mild cognitive impairment, and Alzheimer's disease.

Materials and methods

Subjects

ACR phantom

The American College of Radiology (ACR) magnetic resonance accreditation phantom was used to test for scanner variability. The ACR MR phantom is designed to test a number of parameters, including geometric distortion, spatial resolution, slice thickness and position, interslice gap, estimation of image bandwidth, low contrast detectability, image uniformity, signal to noise ratio, slice offset, and landmark. For more detailed information on this phantom, refer to <http://www.aamp.org/meetings/99AM/pdf/2728-58500.pdf>. The ACR phantom was used because it is widely available and already part of the certification system for scanners. It should be noted that the ADNI phantom is also used each time a subject is scanned in the ADNI study, but it is only scanned with the MP-RAGE sequence and there are no data available with this phantom using the FSE sequence. We asked the specific sites listed in the Acknowledgments to run the ACR phantom for us as an additional scan.

ADNI subjects

Data from 85 subjects (age range = 60–91, average age = 75.47, 44 females, 41 males, $N_{NL} = 32$, $N_{MCI} = 26$, $N_{AD} = 27$) across three vendors (27 Philips, 29 GE, 29 Siemens) was selected from the ADNI database (<http://www.loni.ucla.edu/ADNI>). MMSE scores for each subject were obtained (MMSE_{NC} = 24–30, MMSE_{MCI} = 17–29, MMSE_{AD} = 18–29) (Table 1). Data from 18 ADNI study sites across Canada and the United States were chosen at random for the current study. Multiple scanner brands from each vendor were accepted in the study: GE: Signa Excite, Signa HDx; Philips: Achieva, Intera, Gyroscan Intera, Intera Achieva; Siemens: Sonata, Symphony.

All participants in the ADNI underwent a battery of neuropsychological tests, including the MMSE (Folstein et al., 1975), the CDR-Sum of Boxes (Morris, 1993), and the Global dementia scale (GD-scale) (Auer and Reisberg, 1997; Reisberg et al., 1988). Subjects were clinically assessed for cognitive status and classified as: (a) normal controls with normal cognition and memory, CDR 0, and MMSE between 24 and 30; (b) amnesic MCI with memory complaint verified by a study partner, memory loss measured by education-adjusted performance on the Logical Memory II subscale of the Wechsler Memory Scale-Revised (Wechsler, 1987), preserved activities of daily living, CDR 0.5, MMSE between 24 and 30, and absence of dementia at time of baseline MRI scan; or (c) probable AD with memory complaint validated by an informant, abnormal memory function for age and education level, absence of depression, impaired activities of daily living, diminished cognition, CDR > 0.5, and MMSE between 20 and 26.

Alzheimer's Disease Neuroimaging Initiative

The ADNI is a 5-year non-randomized natural history non-treatment study utilizing data from multiple study centers across the United States and Canada. The primary aim of the ADNI is to examine if serial MRI, PET, biological markers, and clinical and neuropsychological assessments can be combined to analyze the progression of MCI to early AD. The ADNI is a public-private

Table 1

Subject gender breakdown by vendor and diagnostic group (female/male).

Subject enrollment table				
	Philips	GE	Siemens	Total
Normal	6/3	5/13	4/4	15/20
MCI	2/5	7/6	7/4	16/15
AD	4/7	6/4	6/4	16/15
Total	12/15	18/23	17/12	47/50

Table 2

ACR phantom results from 4 scanners. Siemens shows approximately 30 ms prolonged peak T2 compared to GE and Philips. GE showed 10 ms variance between scanners.

ACR phantom peak T2 and histogram width				
	GE HDx	GE Signa Excite	Philips Intera	Siemens Avanto
Peak T2 (ms)	145	135	140	170
T2 histogram width	50	50	50	55

partnership, launched in 2003, funded by the National Institute on Aging, the National Institute of Biomedical Imaging and Bioengineering, the Food and Drug Administration, private pharmaceutical companies, and non-profit organizations.

One of the main goals of the ADNI is to develop optimized methods and uniform standards for the acquisition of multicenter MRI and PET data on normal control subjects and patients with AD and MCI. For more information, refer to <http://www.adni-info.org>.

Image acquisition

For the phantom scans, MRI scanning was performed on four 1.5 T scanners: GE Signa Excite, GE HDx, Philips Intera, and Siemens Avanto. For the ADNI subjects, 1.5 T scanners from General Electric (GE), Philips Medical Systems, and Siemens Medical Solutions were used for examination of tissue from below the base of the cerebellum through the top of the head.

For both the ACR phantom and study participants, the dual fast/turbo spin echo pulse sequence used was acquired in the straight axial plane with the following parameters: effective echo time ($TE_{1\text{eff}}$) = 10.04–13 ms, $TE_{2\text{eff}}$ = 95.22–103 ms, repetition time (TR) = 3000 ms, echo train length (ETL) (turbo factor) = 7–16 (GE = 16, Philips = 10, Siemens = 7* one Siemens subject had an ETL of 13), echo spacing = 12–12.7 ms, slice thickness = 3.0 mm, slice gap = 0 mm, pixel spacing = 0.9375 mm, matrix size = 228–256 × 256. Effective TE was consistent across Philips platforms, but for both GE and Siemens it varied within vendor. Matching parameters between platforms do not produce the same image quality, thus small variations in pulse sequence parameters are often incorporated in large-scale studies. More specific parameter values for each research site can be found at <http://www.loni.ucla.edu/ADNI/Research/Cores>. For simplicity, the pulse sequence will be referred to throughout as FSE, although both Philips and Siemens call it turbo spin echo (Table 2).

Data processing and segmentation

Images from the two echo times, for both phantoms and human subjects, were separated using EFilm (Merge Healthcare, Milwaukee, WI), providing two separate image stacks, one from TE1, the other from TE2. Header information was separated from the images using Image J (<http://www.rsweb.nih.gov/ij/>). Refer to Fig. 1 for a flow diagram of the post-processing steps between the directly-acquired images and the histograms.

The datasets were then analyzed with an in-house computer program using MathCAD 2001i (PTC, Needham, MA) software to generate quantitative-MRI maps (Jara et al., 2006; Suzuki et al., 2006; Jensen et al., 2001). FSE-T2 quantitative maps were generated on a

pixel-by-pixel basis from the two T2-weighted dual echo FSE datasets, according to the mono-exponential function: $T2 = (TE_2 - TE_1) / \ln(S_1/S_2)$, where S_1 and S_2 were the signals obtained at TE_1 and TE_2 , respectively. Fig. 2 shows typical FSE-T2 quantitative maps for NL subjects, MCI subjects, and patients with probable AD.

The brain was segmented using a dual-clustering segmentation algorithm in an in-house MathCAD program (Suzuki et al., 2006; Jara et al., 2006; Jensen et al., 2001). The scans were individually analyzed to obtain the best segmentation of the whole brain and eliminate the inclusion of fat and extra-cranial matter (Fig. 3). Overall the program was able to segment brain tissue from each vendor with no appreciable differences in ease.

Histograms of FSE-T2 relaxation times were generated from the FSE-T2 maps using MathCAD (Fig. 4). The histogram shows an approximately monomodal curve with an asymmetrical tail representing meninges and extra-ventricular CSF. The main peak represents the T2 relaxation time of both gray and white matter (MacKay et al., 2006; Jara et al., 2006).

Statistics

Phantom data were visually analyzed for differences in peak FSE-T2 and histogram width. Statistical analysis was performed on the human data using Excel, Datadesk version 6.1, and SPSS 13. Differences in gender composition between groups were assessed using χ^2 test. Multiple analysis of variance (MANOVA) was used to examine differences between diagnostic groups and platform vendor on peak FSE-T2, FSE-T2 full width at half maximum (T2-width), and volumes for each segment. Scheffe post-hoc analysis was performed on the data. The overall interaction between scanner, diagnosis, and dependent variables was examined with MANOVA with further pairwise comparisons using Scheffe post-hoc analysis. *F*-tests were used to examine variance between scanner vendors for peak FSE-T2 and histogram width. ANOVA with Scheffe post-hoc analysis was performed within scanner vendor to test for differences between NL, MCI, and AD.

Partial correlation analysis was performed to examine relationships between peak FSE-T2, FSE-T2 histogram width, and neuropsychological test scores while controlling for scanner vendor.

Results

ACR phantom

Phantom histograms show differences in peak FSE-T2 between manufacturers ($GE_{\text{HDx}} = 145$ ms, $GE_{\text{Signa Excite}} = 135$ ms, $Philips_{\text{Intera}} = 140$ ms, $Siemens_{\text{Avanto}} = 170$ ms). Histograms of the Siemens scan show approximately 30 ms prolonged peak FSE-T2 compared to the GE and Philips counterparts. Histograms from GE scans show the same average value as the Philips histograms (140 ms), but an approximately 10 ms difference was noted between the 2 GE scanners. Also, Siemens histograms were broader by 5 ms as compared to either GE or Philips (histogram width, $GE_{\text{HDx}} = 50$ ms, $GE_{\text{Signa Excite}} = 50$ ms, $Philips_{\text{Intera}} = 50$ ms, $Siemens_{\text{Avanto}} = 55$ ms).

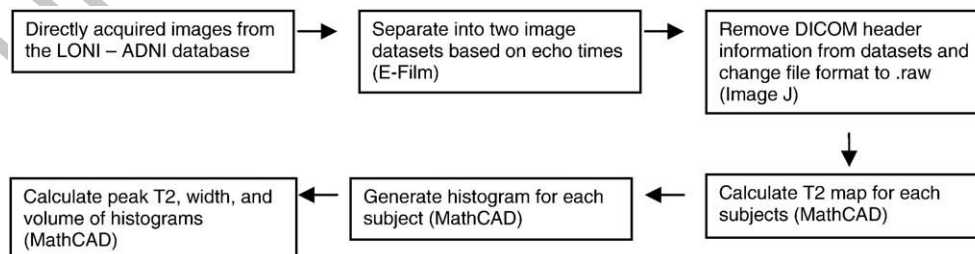


Fig. 1. Flow chart showing the post-processing data analysis used to obtain histograms from the directly-acquired images.

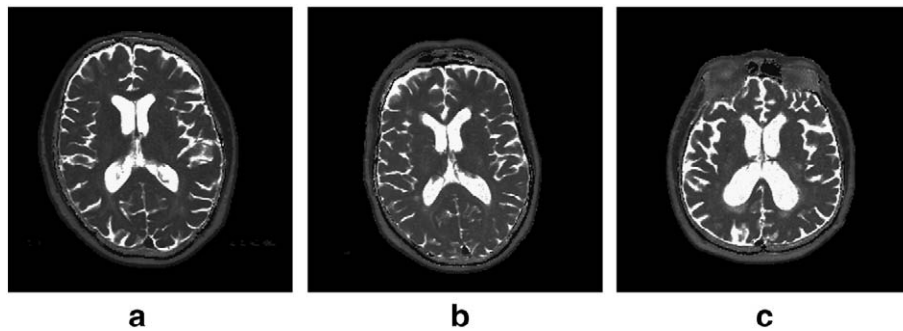


Fig. 2. Representative T2 quantitative MR maps. a) T2 map of a 79 year old male control subject on a GE Signa Excite platform. b) T2 map of a 77 year old female subject with MCI scanned on a Siemens Sonata platform. c) Shows a T2 map from a 75 year old male AD subject scanned with a Siemens Avanto platform.

276 ADNI subjects

277 Age and gender were not significantly different amongst diagnos-
278 tic groups or scanner vendors ($p > 0.05$). Average histograms were
279 created according to vendor and subject population (Fig. 5).

280 Peak FSE-T2

281 Overall analysis showed a significant difference between scanner
282 vendors ($F_{2, 73} = 146.37, p < 0.0001$). Follow up comparisons
283 revealed Siemens peak FSE-T2 was 15–29 ms ($p < 0.0001$) longer
284 than both GE and Philips across the three diagnostic groups (Fig. 5).
285 GE peak values were on average 4 ms prolonged over Philips values;
286 however, this did not reach significance possibly due to the larger
287 degree of variance seen across GE subjects.

288 Within GE platforms no significant differences were found for peak
289 FSE-T2. The directionality of change in GE indicated a decrease in FSE-T2
290 from NL to MCI, an increase in FSE-T2 from MCI to AD, and an increase in
291 FSE-T2 from NL to AD. Within Philips platforms, no significant
292 differences were found for peak FSE-T2. The directionality of change
293 in Philips shows an increase in peak FSE-T2 from NL to MCI, a decrease in
294 peak FSE-T2 from MCI to AD, and a decrease in peak FSE-T2 from NL to
295 AD. Within Siemens platforms a significant difference was found for
296 peak FSE-T2 between NL and MCI ($p > 0.05$), but not between NL and AD
297 subjects. The directionality of peak FSE-T2 change in Siemens indicates a
298 decrease from NL to MCI, an increase from MCI to AD, and a decrease
299 from NL to AD.

300 Tests of variance indicate that Philips ($s^2 = 7.764$) scanners show
301 significantly lower variance than either GE ($s^2 = 38.239$) ($p < 0.001$) or
302 Siemens ($s^2 = 30.988$) ($p < 0.001$) for peak FSE-T2. GE and Siemens
303 variance for peak FSE-T2 was not significantly different ($p > 0.05$).

304 FSE-T2 histogram width

305 The width of the histogram reflects the homogeneity of tissue
306 composition. Width was measured at half maximum for each FSE-T2



Fig. 3. Representative example of segmented brain tissue using a dual-clustering segmentation algorithm. a) The brain tissue included in the segmentation is represented in the highlighted region. b) Segmented brain.

281 histogram. Overall analysis showed significant scanner differences ($F_{2, 73} = 9.483, p < 0.0001$). ANOVA revealed a significant difference
282 between Siemens and both Philips and GE ($p < 0.005$).
283

Correlations

284 Peak FSE-T2 and FSE-T2 width were assessed for correlations with
285 age, CDR, MMSE, and GD scale scores. Peak FSE-T2 was found to
286 significantly correlate with age ($r = 0.370, p < 0.01$). FSE-T2 histogram
287 width was significantly correlated with GD scale ($r = 0.232, p < 0.05$).
288

Discussion

289 The specific goals of this work were to identify potential vendor-
290 dependent systematic differences in quantitative FSE-T2 maps of the
291 ACR phantom and human brain and to study FSE-T2 histogram
292 properties across the spectrum of normal aging, MCI, and AD.
293 Significant overall differences were found between scanner vendors
294 across the FSE-T2 histogram-derived parameters in both phantom
295 and human studies. Follow up analysis showed that Siemens had
296 higher FSE-T2 peak values and broader histograms than GE and
297 Philips. Measurements were not statistically significant between
298 diagnostic groups when accounting for scanner vendor, which
299 decreased the effective sample size per group to between 7 and 18
300 subjects. The small sample size within vendors may partially account
301 for there not being a significant difference between peak FSE-T2 of AD,
302 MCI, and normal aging subjects.
303

304 The trends between NL, MCI, and AD, suggest a scanner vendor-
305 disease interaction effect, such that the trend for FSE-T2 between
306 normal aging, MCI, and AD was inconsistent between vendors (i.e.
307 normal aging from one vendor produced prolonged T2 compared to
308 AD, while in another vendor we observed the opposite trend). These
309 interactions are of greatest concern and will need to be verified with a
310 larger sample. If true, this suggests that combining data from different
311 vendors in one analysis, even when using co-factors, will end up
312 masking the underlying effect.
313

314 Peak FSE-T2 was shown to correlate with age, consistent with the
315 results of a previously published study (Laakso et al., 1996).
316 Histogram width correlated with GD scale. Histogram width reflects
317 water environment inhomogeneity (Whittall et al., 1997), indicating
318 that brain tissue becomes more heterogeneous as the severity of
319 dementia measured by the GD scale increases.
320

321 Variability between sites indicates that there was a larger degree of
322 variance between GE and Siemens sites. The variability between sites
323 using GE scanners was also observed in the phantom scans. Although
324 GE was the only vendor for which the phantom was scanned on more
325 than one platform. Additional phantom scans on Philips and Siemens
326 platforms would be useful to help confirm the degree of variance
327 between scanners.
328

329 Peak FSE-T2, for both phantom and human subjects, was at least
330 20–30 ms prolonged with Siemens' histograms compared to GE and
331

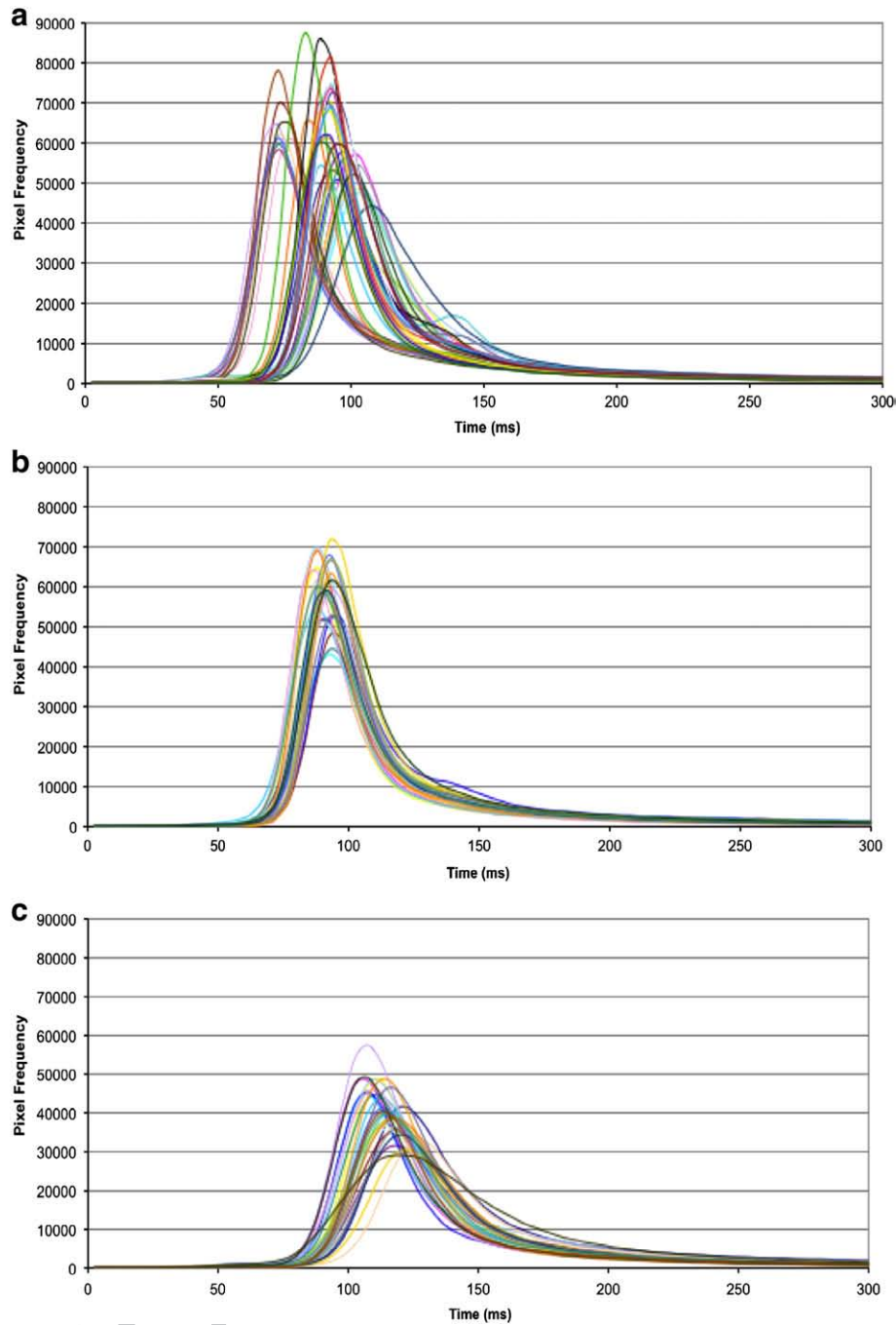


Fig. 4. ICM T2 histograms from all subjects and scanner platforms, a) Philips b) GE and c) Siemens.

354 Philips. The FSE pulse sequences used in the ADNI were not
 355 standardized between research sites, consistent with protocols of
 356 many other large-scale studies including the Framingham Heart Study
 357 (DeCarli et al., 2005), MIRAGE (Cuenco et al., 2008), and many clinical
 358 drug trials.

359 This study poses a few limitations related to pulse sequence
 360 parameters and scanner hardware and software. Because the
 361 sequences were not completely standardized between all platforms,
 362 some scans were acquired with different effective TE or ETL. The signal
 363 intensity with T2 is primarily controlled by echo time. Effective TE
 364 may differ between vendors based on the k-space acquisition scheme,
 365 which may have induced some of the observed scanner-related
 366 variance. Much of the inaccuracy of FSE-T2 is due to stimulated echo,
 367 which is affected by both ETL (turbo factor) and echo spacing. The
 368 observed difference in FSE-T2 may be inherent to the vendor-specific

scheme used to acquire k-lines with the fast spin echo readout, slice
 369 profile, and phase encoding order. Other factors, such as the coils, BO
 370 and B1 inhomogeneities (Majumdar et al., 1986b; Poon and Henkel-
 371 man, 1992), RF pulse imperfections (Majumdar et al., 1986a), and
 372 temperature variations, could also contribute to the scanner-related
 373 variance. 374

Whole brain histogram-derived FSE-T2 measures may not be
 375 sensitive enough to detect AD-related changes; however, T2 has been
 376 shown to regionally differ in AD and MCI compared to normal aging
 377 (Englund et al., 1987; Kirsch et al., 1992; Laakso et al., 1996; Pitkanen
 378 et al., 1996; Parsey and Krishnan, 1998; Wang et al., 2004; Schenck
 379 et al., 2006; Arfanakis et al., 2007). A potential area for future research
 380 is to examine T2 relaxation times using voxel-based relaxometry
 381 (VBR), which has been used to show T2 changes in autism (Hendry
 382 et al., 2006), epilepsy (Pell et al., 2004; Pell et al., 2008) and multiple
 383

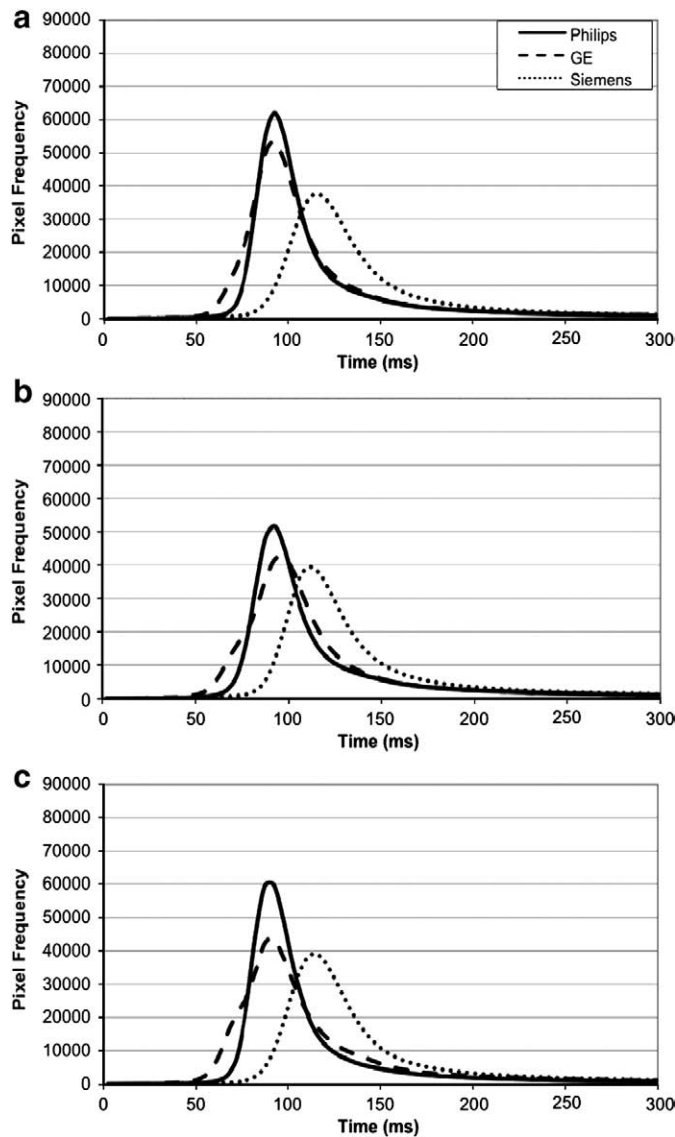


Fig. 5. Quantitative ICM T2 histogram averaged within scanner vendor: Philips, GE, and Siemens. The slight bimodal nature of the GE curve represents those subjects from site 005, which had average values approximately 20 ms lower than other GE sites. a) Normal control subjects: Philips and GE peak at 97.35 and 98.37 while Siemens peaks at 119.69 ms. The width of the spectrum is approximately 50.6 for Philips, GE, and Siemens respectively. b) MCI subjects: Philips peak T2 = 94.29 ms, GE peak = 99.38 ms, while Siemens peaks at 119.09 ms. The width of the spectrum is 52, 53, and 55 U for Philips, GE, and Siemens respectively. c) AD subjects: Philips peak = 95.68 ms, GE peak = 102.08, and Siemens peak = 116.75 ms. The width of the spectrum is 51, 53, and 54 for Philips, GE, and Siemens respectively.

system atrophy of the cerebellar type (Specht et al., 2005; Minnerop et al., 2007).

Future studies that seek to utilize quantitative FSE-T2 measures will need to standardize the pulse sequence across scanners or devise a post-processing method to standardize measures. Alternatively, small fluid-filled objects with known T2 values could be scanned alongside each subjects' head to provide reference signal (House et al., 2006). Using other sequences may also help us to understand some of the differences between how each vendor handles the processing of T2 based imaging, but since these are not generally used in multi-site studies it is difficult to say how this will help us to understand the differences we have found using the FSE sequence.

This study used MRI and neuropsychological test ADNI data across NL, MCI and AD subjects. MRI data acquired with GE, Philips, and Siemens scanners to examine which properties of FSE-T2 quantitative

MRI may be useful for the classification of MCI and early AD. Significant quantitative FSE-T2 differences were found between vendors in peak FSE-T2 and histogram width. The results herein suggest that FSE-T2 histogram measures can vary significantly with scanner vendor. Specifically, Siemens data consistently produced higher peak FSE-T2 values and broader histogram widths than either GE or Philips. The second purpose was to examine T2 histograms within normal aging, MCI, and AD over the whole brain. Few significant differences were found between diagnostic groups and the observed trends were inconsistent amongst the represented vendors, suggesting a potential scanner-disease interaction. The differences in scanner overshadowed the potential influence of subject diagnostic group on FSE-T2 measures. Significant correlations between peak FSE-T2 and FSE-T2 histogram width with global scale of dementia and measures of memory and cognitive functioning were observed.

To the authors' knowledge, a multi-site study involving quantitative FSE-T2 datasets from GE, Philips, and Siemens has not been reported in previous literature. The results obtained in this study should serve to encourage increased quality control for measures of FSE-T2 related scans in large-scale studies utilizing data from multiple scanner platforms. They also point out potential differential effects of scanner brand that may not be adequately controlled by adding a covariate to a statistical analysis.

Conclusion

The aim of this study was to assess the utility of FSE-T2 quantitative MRI of the brain for the diagnosis of AD and its early manifestations. The results indicate that FSE-T2 measures can vary significantly between scanner platforms and that FSE-T2 quantitative-MRI image processing algorithms which include the platform specific magnetization dynamic effects during the FSE readouts are needed for reconciling multi-platform FSE-T2 measurements. Despite these differences, overall FSE-T2 relaxation properties were related to the global dementia status of the subjects.

Uncited references

Jack et al., 2008
Mueller et al., 2005
Petersen et al., 2005

Acknowledgments

The Foundation for the National Institutes of Health (<http://www.fnih.org>) coordinates the private sector participation of the \$60 million ADNI public-private partnership that was begun by the National Institute on Aging (NIA) and supported by the National Institutes of Health. To date, more than \$27 million has been provided to the Foundation for NIH by Abbott, AstraZeneca AB, Bayer Schering Pharma AG, Bristol-Myers Squibb, Eisai Global Clinical Development, Elan Corporation, Genentech, GE Healthcare, GlaxoSmithKline, Innogenetics, Johnson & Johnson, Eli Lilly and Co., Merck & Co., Inc., Novartis AG, Pfizer Inc., F. Hoffmann-La Roche, Schering-Plough, Synarc Inc., and Wyeth, as well as non-profit partners the Alzheimer's Association and the Institute for the Study of Aging.

We would also like to thank Clifford Jack, Bret Borowski, Earl Zimmerman, and John Cowan for their assistance scanning the ACR phantom.

References

Arfanakis, K., Gui, M., Tamhane, A.A., Carew, J.D., 2007. Investigating the medial temporal lobe in Alzheimer's disease and mild cognitive impairment, with TurboProp diffusion tensor imaging, MRI-volumetry, and T2-relaxometry. *Brain Imaging Behav.* 1, 11–21.

- 457 Auer, S., Reisberg, B., 1997. The GDS/FAST staging system. *Int. Psychogeriatr.* 9 (Suppl. 1),
458 167–171.
- 459 Bartzokis, G., Beckson, M., Hance, D.B., Marx, P., Foster, J.A., Marder, S.R., 1997. MR
460 evaluation of age-related increase of brain iron in young adult and older normal
461 males. *Magn. Reson. Imaging* 15, 29–35.
- 462 Cuenco, K.T., Green, R.C., Shang, J., Lunetta, K., Erlich, P.M., Cupples, L.A., Farrer, L.A.,
463 DeCarli, C., for the MIRAGE Study Group, 2008. Magnetic resonance imaging traits
464 in siblings discordant for Alzheimer disease. *J. Neuroimaging* 18, 268–275.
- 465 DeCarli, C., Massaro, J., Harvey, D., Hald, J., Tullberg, M., Au, R., Beiser, A., D'Agostino, R.,
466 Wolf, P.A., 2005. Measures of brain morphology and infarction in the Framingham
467 heart study: establishing what is normal. *Neurobiol. Aging* 26, 491–510.
- 468 Deoni, S.C.L., Williams, S.C.R., Jezzard, P., Suckling, J., Murphy, D.G.M., Jones, D.K., 2008.
469 Standardized structural magnetic resonance imaging in multicentre studies using
470 quantitative T1 and T2 imaging at 1.5 T. *NeuroImage* 40, 662–671.
- 471 Englund, E., Brun, A., Persson, B., 1987. Correlations between histopathologic white matter
472 changes and proton MR relaxation times in dementia. *Alzheimer Dis. Assoc. Disord.* 1,
473 156–170.
- 474 Fu, L., Fonov, V., Pike, B., Evans, A.C., Collins, D.L., 2006. Automated analysis of multi site
475 MRI phantom data for the NHPD project. *Med Image Comput Comput Assist Interv* 9 (part2), pp. 144–151.
- 476 Hendry, J., DeVito, T., Gelman, N., Densmore, M., Rajakumar, N., Pavlosky, W., Williamson,
477 P.C., Thompson, P.M., Drost, D.J., Nicolson, R., 2006. White matter abnormalities in
478 autism detected through transverse relaxation time imaging. *NeuroImage* 29,
479 1049–1057.
- 480 House, M.J., St. Pierre, T.G., Foster, J.K., Martins, R.N., Clarmette, R., 2006. Quantitative MR
481 imaging R2 relaxometry in elderly participants reporting memory loss. *AJNR* 27,
482 430–439.
- 483 Ihalainen, T., Sipilä, O., Savolainen, S., 2004. MRI quality control: six imagers studied using
484 eleven unified image quality parameters. *Eur. J. Radiol.* 14, 1859–1865.
- 485 Jack Jr., C.R., 1996. Hippocampal T2 relaxometry in epilepsy: past, present, and future.
486 *AJNR* 17, 1811–1814.
- 487 Jack Jr., C.R., Bernstein, M.A., Fox, N.C., Thompson, P., Alexander, G., Harvey, D., Borowski, B.,
488 Britson, P.J., Whitwell, J.L., Ward, C., Dale, A.M., Felmlee, J.P., Gunter, J.L., Hill, D.L.G.,
489 Killiany, R., Schuff, N., Fox-Bosetti, S., Lin, C., Studholme, C., DeCarli, C.S., Krueger, G.,
490 Ward, H.A., Metzger, G.J., Scott, K.T., Mallozzi, R., Blezek, D., Levy, J., Debbins, J.P.,
491 Fleisher, A.S., Albert, M., Green, R., Bartzokis, G., Glover, G., Mugler, J., Weiner, M.W.,
492 for the ADNI Study, 2008. The Alzheimer's Disease Neuroimaging Initiative (ADNI): MRI
493 methods. *J. Magn. Reson. Imaging* 27, 685–691.
- 494 Jara, H., Sakai, O., Mankal, P., Irving, R., Norbash, A.M., 2006. Multispectral quantitative
495 magnetic resonance imaging of brain iron stores. *Top. Magn. Reson. Imaging* 17,
496 19–30.
- 497 Jensen, M.E., Caruthers, S.D., Jara, H., 2001. Quantitative magnetic resonance imaging with
498 the mixed turbo spin-echo pulse sequence: a validation study. *Internet J. Radiol.* 2
499 Available from: http://www.ispub.com/journal/the_internet_journal_of_radiology.html.
- 500 Kirsch, S.J., Jacobs, R.W., Butcher, L.L., Beatty, J., 1992. Prolongation of magnetic resonance
501 T2 time in hippocampus of human patients marks the presence and severity of
502 Alzheimer's disease. *Neurosci. Lett.* 134, 187–190.
- 503 Laakso, M.P., Partane, K., Soininen, H., Lehtovirta, M., Hallikainen, M., Hanninen, T., Helkala,
504 E.L., Vainio, P., Reikkinen Sr., P.J., 1996. MR T2 relaxometry in Alzheimer's disease and
505 age-associated memory impairment. *Neurobiol. Aging* 17, 535–540.
- 506 MacKay, A., Laule, C., Vavasour, I., Bjarnason, T., Kolind, S., Madler, B., 2006. Insights into
507 brain microstructure from the T2 distribution. *Magn. Reson. Imaging* 24, 515–525.
- 508 Majumdar, S., Orphanoudakis, S.C., Gmitro, A., O'Donnell, M., Gore, J.C., 1986a. Errors in the
509 measurements of T2 using multiple-echo MRI techniques: 1. Effect of radiofrequency
510 pulse imperfections. *Magn. Reson. Med.* 3, 397–417.
- 511 Majumdar, S., Orphanoudakis, S.C., Gmitro, A., O'Donnell, M., Gore, J.C., 1986b. Errors in the
512 measurements of T2 using multiple-echo MRI techniques: 2. Effects of static field
513 inhomogeneity. *Magn. Reson. Med.* 3, 562–574.
- 514 Minnerop, M., Specht, K., Ruhlmann, J., Schimke, N., Abele, M., Weyer, A., Wullner, U.,
515 Klockgether, T., 2007. Voxel-based morphometry and voxel-based relaxometry in
516 multiple system atrophy – a comparison between clinical subtypes and correlations
517 with clinical parameters. *NeuroImage* 36, 1086–1095.
- 518 Mueller, A.G., Weiner, M.W., Thal, L.J., Petersen, R.C., Jack, C.R., Trojanowski, J.Q., Toga, A.W.,
519 Beckett, L., 2005. Ways toward an early diagnosis in Alzheimer's disease: the
520 Alzheimer's Disease Neuroimaging Initiative (ADNI). *Alzheimers Dement.* 1, 55–66.
- 521 Parsey, R.V., Krishnan, K.R.R., 1998. Quantitative analysis of T2 signal intensities in
522 Alzheimer's disease. *Psychiatry Res.* 82, 181–185.
- 523 Pell, G.S., Briellmann, R.S., Waites, A.B., Abbott, D.F., Jackson, G.D., 2004. Voxel-based
524 relaxometry: a new approach for analysis of T2 relaxometry changes in epilepsy.
525 *NeuroImage* 21, 707–713.
- 526 Pell, G.S., Briellmann, R.S., Pardoe, H., Abbott, D.F., Jackson, G.D., 2008. Composite voxel-
527 based analysis of volume and T2 relaxometry in temporal lobe epilepsy. *NeuroImage*
528 39, 1151–1161.
- 529 Petersen, R., Albert, M., DeKosky, S., Salmon, D., Snyder, P., Tariot, P., 2005. The Alzheimer's
530 Disease Neuroimaging Initiative Protocol (ADNI). <http://www.adni-info.org/> last
531 accessed June 2008.
- 532 Pitkanen, A., Laakso, M., Kiilviainen, R., Partanen, K., Vainio, P., Lehtovirta, M., Reikkinen Sr., P.,
533 Soininen, H., 1996. Severity of hippocampal atrophy correlates with the prolongation of
534 MRI T2 relaxation time in temporal lobe epilepsy but not in Alzheimer's disease.
535 *Neurology* 46, 1724–1730.
- 536 Poon, C.S., Henkelman, R.M., 1992. Practical T2 quantitation for clinical applications. *J. Magn.*
537 *Reson. Imaging* 2, 541–553.
- 538 Reisberg, B., Ferris, S.H., de Leon, M.J., Crook, T., 1988. Global Deterioration Scale (GDS).
539 *Psychopharmacol. Bull.* 24, 661–663.
- 540 Schenck, J.F., Zimmerman, E.A., Li, Z., Adak, S., Saha, A., Tandon, R., Fish, K., Belden, C., Gillen,
541 R.W., Barba, A., Henderseon, D.L., Neil, W., O'Keefe, T., 2006. High-field Magn. Reson.
542 Imaging of brain iron in Alzheimer disease. *Top. Magn. Reson. Imaging* 17, 41–50.
- 543 Specht, K., Minnerop, M., Muller-Hubenthal, J., Klockgether, T., 2005. Voxel-based analysis
544 of multiple-system atrophy of the cerebellar type: complementary results by
545 combining voxel-based morphometry and voxel-based relaxometry. *NeuroImage*
546 25, 287–293.
- 547 Stonnington, C.M., Tan, G., Kloppel, S., Chu, C., Dragnakxi, B., Jack Jr., C.R., Chen, K.,
548 Ashburner, J., Frackowiak, R.S.J., 2008. Interpreting scan data acquired from multiple
549 scanners: a study with Alzheimer's disease. *NeuroImage* 39, 1180–1185.
- 550 Suzuki, S., Sakai, O., Jara, H., 2006. Combined volumetric T1, T2, and secular-T2 quantitative
551 MRI of the brain: age-related global changes (preliminary results). *Magn. Reson.*
552 *Imaging* 24, 877–887.
- 553 Vymazal, J., Brooks, R.A., Baumgarner, C., Traun, V., Katz, D., Bulte, J.W.M., Bauminger, E.R.,
554 Di Chiro, G., 1996. The relation between brain iron and NMR relaxation times: an
555 invitro study. *Magn. Reson. Med.* 35, 56–61.
- 556 Wang, H., Yuan, H., Shu, L., Xie, J., Zhang, D., 2004. Prolongation of T2 relaxation times of
557 hippocampus and amygdala in Alzheimer's disease. *Neurosci. Lett.* 363, 150–153.
- 558 Whittall, K.P., MacKay, A.L., Graeb, D.A., Nugent, R.A., Li, D.K.B., Paty, D.W., 1997. In vivo
559 measurement of T2 distributions and water contents in normal human brain. *Magn.*
560 *Reson. Med.* 37, 34–43.
- 561
562